

Det Kongelige Danske Videnskabernes Selskab

Matematisk-fysiske Meddelelser, bind **26**, nr. 10

Dan. Mat. Fys. Medd. **26**, no.10 (1951)

SYNCHRONISATION OF AIR-JET
GENERATORS WITH AN APPENDIX ON
THE STEM GENERATOR

BY

JUL. HARTMANN AND ERIK TRUDSØ



København

i kommission hos Ejnar Munksgaard

1951

Printed in Denmark
Bianco Lunos Bogtrykkeri

Introduction.

The present paper deals with the problem of synchronising acoustic generators of the air-jet type, the so-called Hartmann generators. The generator proper has so often been described¹ that we may here confine ourselves to a brief review of its principle and of its performance. Fig. 1 will explain the principle. N is a nozzle from which an air-jet of a velocity exceeding that of sound is emitted. In front of N is arranged a cylindrical oscillator O , of a diameter d and a depth l which are both normally equal to the diameter d_0 of the jet orifice. If the aperture of the nozzle is adjusted within one or other of a series of jet-intervals, the intervals of instability, which follow each other equidistantly out along the jet, then, and then only, the air in the oscillator will vibrate and the oscillator will emit waves. The frequency of these waves is of the same order of size as the natural frequency of the oscillator, increasing, however, somewhat with the distance a between the nozzle N and the aperture of the oscillator. The acoustic power emitted is comparatively very high. It depends on the frequency N_m corresponding to optimal efficiency of the generator, according to the formula

$$(1) \quad I = 14.6 \cdot 10^9 \cdot \frac{1}{N_m^2} \text{ Watt.}$$

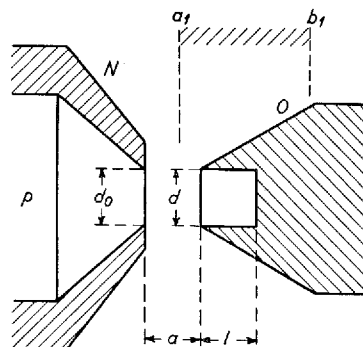


Fig. 1. Principle of the Acoustic Air-Jet Generator.

¹ Reference may be made to the monograph: The Acoustic Air-Jet Generator. Ingeniørvideenskabelige Skrifter No. 4. 1939 issued by The Academy of Technical Sciences, Copenhagen.

From (1) the following figures are derived:

N_m . . .	1000	5000	10000	20000	50000	100000	Hz
I	14600	585	146	36.5	5.85	1.46	Watt

It will be gathered that wave fields of larger intensities cannot be created by one single generator. Now in certain applications of the waves, particularly in that of smoke precipitation, it would seem highly desirable to produce homogeneous fields of high frequency and large intensity and extension. This consideration suggested an attempt at synchronising air-jet generators, for if such synchronisation could be achieved then it would be an easy matter to produce fields of the description called for by suitably arranged generators. The problem of synchronisation was long postponed; it was not until after the last war that it could be tackled seriously with the result reported below.

1. Earlier Experiments.

Some occasional experiments had, however, preceded the research work here dealt with. Some of these may be described. A very fine experiment showing the effect of synchronous waves on the emission of a generator was carried out as follows. Laterally to the generator in fig. 1 a small piece of sheet iron could

be displaced. If its distance was varied, a very marked influence of the reflected waves on the emission became manifest. In order to make it visible, the generator was arranged on an optical bench according to the method of striæ. It is known from the monograph referred to above, that the vibrations of the air in the oscillator can be directly observed and their amplitude estimated from the width of the band drawn in front of the oscillator by the "Riemann mirror" following the motion of the vibrating air. Fig. 2 shows the aspect of the band. Its width, i. e. the double amplitude

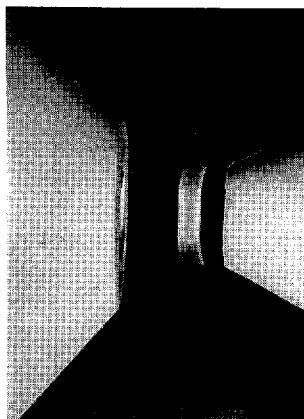


Fig. 2. Vibrations of an Oscillator made visible by Means of the Riemann Mirror.

could be controlled by the reflector indicated above, or the vibrations could be stopped altogether with the reflector at a suitable distance.

Experiments on twin generators were carried out by means of the two apparatus shown in figs.3 and 4. Between two co-axial

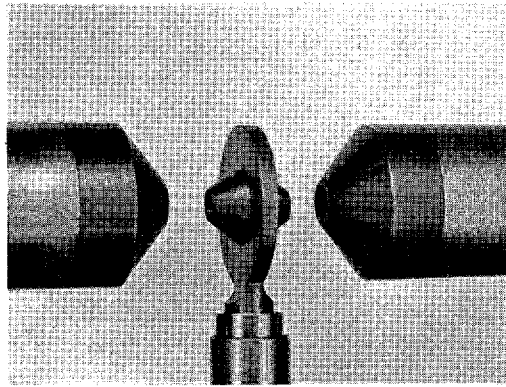


Fig. 3. Twin Generator with directly coupled Oscillators.

nozzles, the interspace of which could be varied, a twin oscillator could be centered and displaced axially. In the apparatus seen in fig. 3 the twin oscillator simply formed a cylindrical bore right through the material. When properly adjusted the twin generator would emit waves of a frequency corresponding to an oscillator of a depth equal to half the length of the bore. In the apparatus

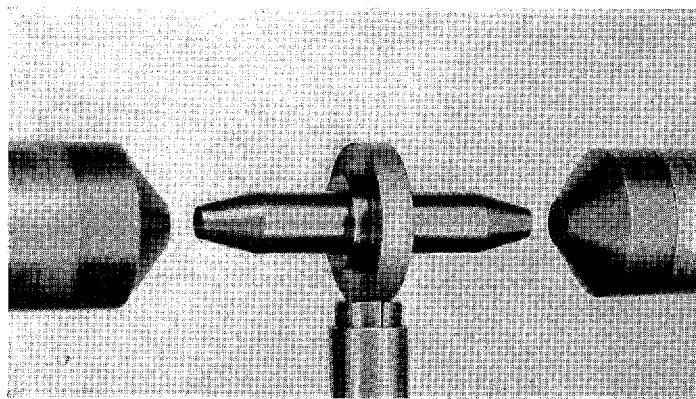


Fig. 4. Twin Generator with Oscillators coupled through the exterior Wave Field.

shown in fig. 4 the two oscillators were independent of each other but it proved an easy matter to adjust the twin oscillator so that the waves emitted from both of the components were synchronised through the coupling by the surrounding air.

Finally attention should be drawn to an early attempt to greatly increase the absolute output at high frequencies by means of a generator based on a disk shaped air-jet of supersonic

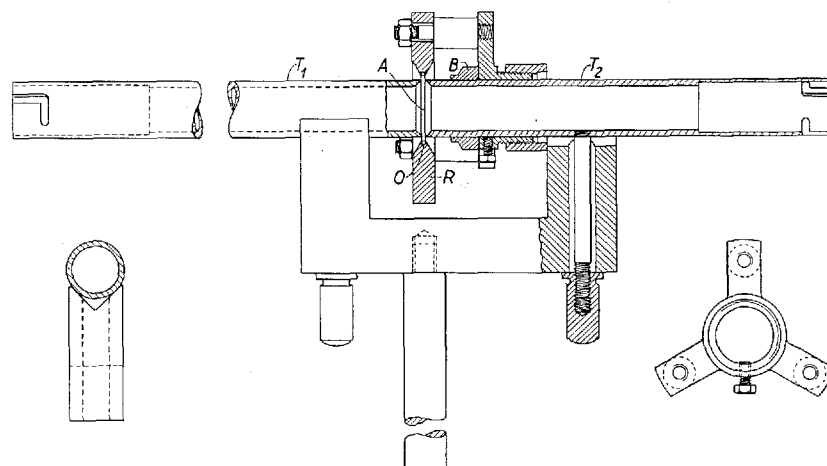


Fig. 5. The Disk-Jet Generator.

velocity, the so-called disk-jet generator. Its substantiation will be understood from fig. 5. The cylindrical bore of the normal generator is here replaced by an annular slit A between the sharpened edges of two co-axial tubes T_1 and T_2 through which compressed air is passed to the slit. With this arrangement a disk shaped air-jet with a velocity exceeding that of sound is produced and in accordance herewith the oscillator is given the form of a rectangular groove O in the wedge-shaped edge of a ring. The ring is adjusted so that its plane of symmetry coincides with that of the annular slit, and further so that the axis of the ring coincides with that of the tubes. The means for this adjustment will appear from fig. 5. In particular attention should here be called to the ring B which fits on to the tube T_2 and can be displaced on the latter. The ring is furnished with a recess fitting the oscillator accurately, and so suited for making the latter member co-axial with the tubes. Fig. 5 also illustrates the way in

which the two tubes are made co-axial and further the clamping of the tubes on the support. Fig. 6 shows a photograph of the generator. Again, fig. 7 is a reproduction of a photograph of part

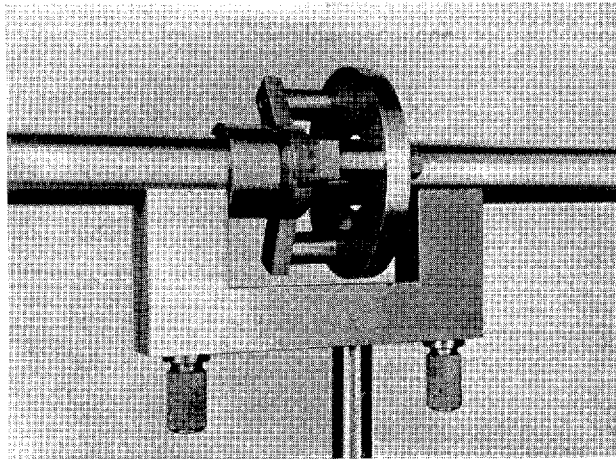


Fig. 6. The Disk-Jet Generator.

of the disk-jet obtained by the method of striæ. The periodic structure of the jet is manifest.

The great question with regard to the disk-jet generator was, whether it would prove possible to make the air in the annular

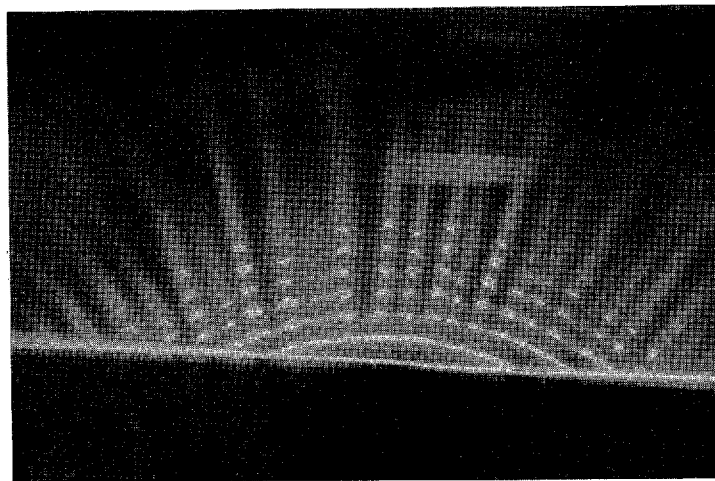


Fig. 7. Part of the Disk-Jet photographed by the Method of Striæ.

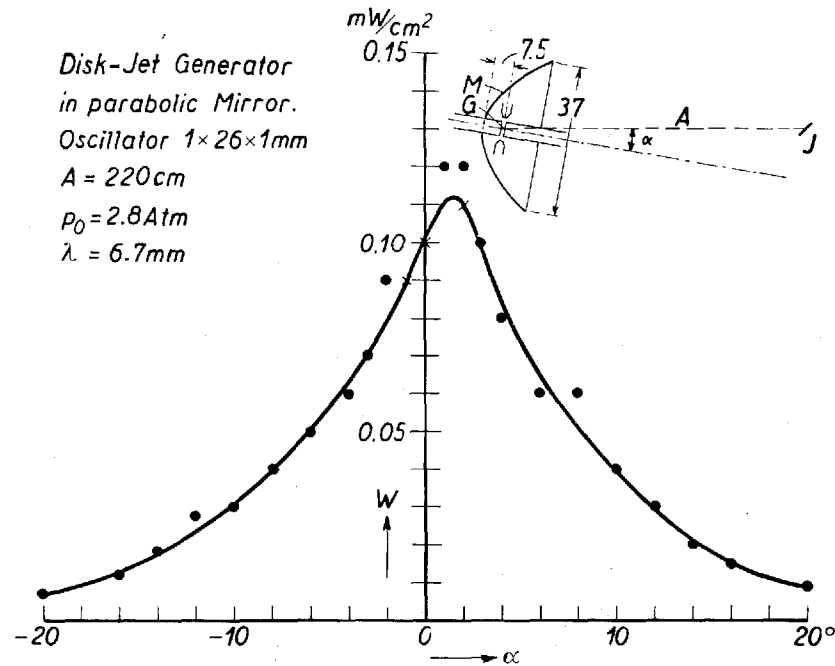


Fig. 8. Angular Distribution of the Radiation from the Disk-Jet Generator mounted in a parabolic Mirror.

oscillator vibrate synchronously all round the circumference of the oscillator. For this, as will be understood, is a first condition for the utility of the generator. In order to settle this question the generator was arranged in the focus of a parabolic mirror of aperture 37 cm and focal length 7.5 cm, the generator being made co-axial with the mirror as indicated in fig. 8. The distribution of the radiation was investigated in the space in front of the generator, and the total radiation was computed from the results. The latter are reproduced in fig. 8. Again, measurement was made of the total radiation from an ordinary air-jet generator with cylindrical jet and oscillator arranged in the focus of the same mirror and emitting a radiation of the same wave-length as the disk-jet generator. Fig. 9 is a picture of the angular distribution of this radiation. Hereafter the two total radiations were compared and the ratio was found to be 20, i. e. the radiation from the disk-jet generator in the mirror is 20 times that of the ordinary generator in the same mirror. This result undoubtedly suggests

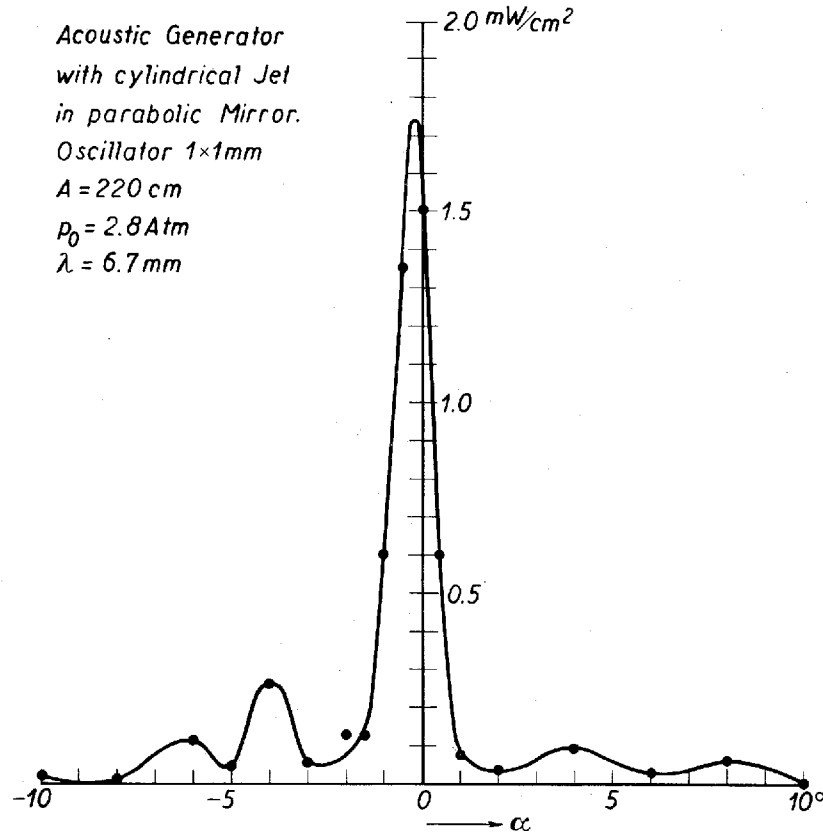


Fig. 9. Angular Distribution of the Radiation from an ordinary Air-Jet Generator mounted in a parabolic Mirror.

a fairly perfect synchronisation judging also from the following estimate.

With the ordinary generator the radiation is emitted from a cylindrical surface the size of which is proportional to the circumference πd of the jet of diameter d . In the case of the disk-jet generator the radiating surface is proportional to $2 \cdot \pi D$, where D is the diameter of the tube with the annular slit. The factor 2 corresponds to the two directions in which radiation takes place. The ratio of the radiations for the two generators may, in the case of the same wave-length, reasonably be expected to be $\frac{2\pi D}{\pi d} = \frac{2D}{d}$. In our case $D = 22 \text{ mm}$ and $d = 1 \text{ mm}$, corresponding to radiations of wave-length 6.7 mm . So $2D/d = 44$.

Although this figure is more than twice that of the actual ratio for the radiations as found in connection with a parabolic mirror, the comparatively high value of the latter ratio undoubtedly speaks in favour of a rather complete synchronisation. In fact a value of the ratio well below the "theoretical" must be anticipated, seeing that the concentration of the radiation with the disk-jet

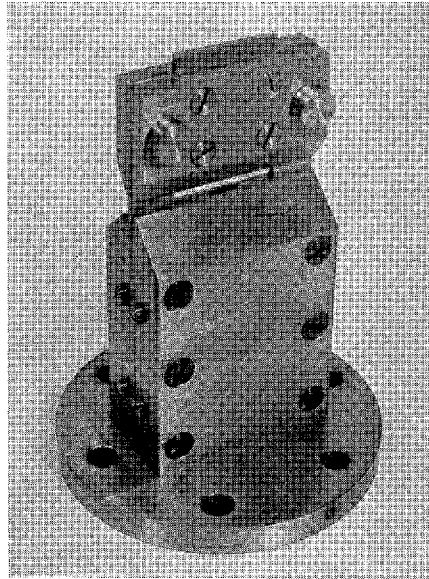


Fig. 10. Generator with a laminar Jet.

generator, is incontestably less perfect than with the cylindrical jet generator owing to the many reflecting surfaces with the former generator. Otherwise the "theory" for the ratio of the two radiations is of course very crude. In this connection the powers required for the maintenance of the disk-jet and the cylindrical jet may be compared. At the same excess pressure 2.8 Atm., they are as the areas of the apertures. For the disk-jet the area was $\pi \cdot 22 \cdot 0.9$ while for the cylindrical jet it was $\frac{\pi}{4} \cdot 1^2$. So the ratio is $88 \cdot 0.9 = 79$. This means that the practical efficiency of the disk-jet generator is about 4 times less than that of the ordinary generator. So the sole raison d'être for the former generator is that a much larger output is available.

It may further be stated that the absolute figures for the radiations from the two arrangements compared above were found to be:

Disk-Jet Generator 50 Watt

Normal Generator 2.4 Watt.

Here the absorptions in the air and in the curtains of gauze protecting the Rayleigh disk indicator from the stream of air from

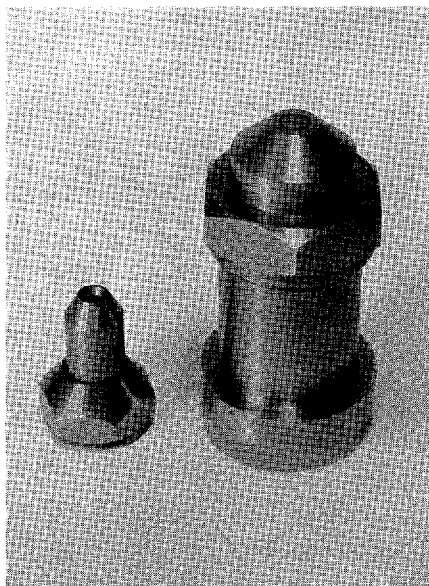


Fig. 11. Generator with a hollow cylindrical Jet.

the generators are eliminated. The common wave-length of the two generators was $\lambda = 6.7$ mm. Hence the frequency was about 51000 Hz. At that frequency the total radiation from a normal generator (not mounted in a mirror) should, according to the formula (1), be 5.64 Watt, thus somewhat more than twice the power "rectified" by the parabolic mirror.

For the sake of completeness two still earlier attempts at increasing the absolute output of the air-jet generator may be mentioned. Fig. 10 shows a generator with a laminar jet and a corresponding oscillator and fig. 11 a generator with a hollow cylindrical jet. The design of both of the two apparatus will appear from the figures. None of them would seem to possess particular merits except perhaps in connection with special problems.

2. Synchronisation Experiments with adjustable Twin-Generators.

The experiments so far described may be considered as a preliminary approach to the main subject of the present paper viz. the study of the conditions for synchronisation of separate air-jet generators. The first experiment on such generators was carried out with an apparatus of the same type as that shown in fig. 4. Since, however, it was recognised that the conditions for synchronisation comprise a more or less definite distance

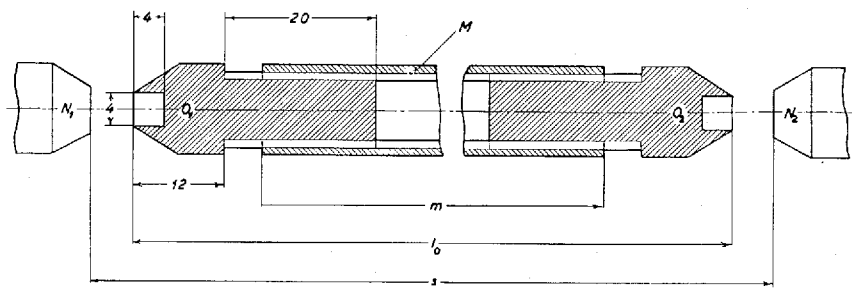


Fig. 12. Twin Generator with variable Distance between the Oscillators and independent Setting of the same.

between the two oscillators, and seeing that means should preferably be provided for setting each oscillator relatively to its nozzle independently of the position of the other, the actual apparatus was designed as indicated in fig. 12. The two oscillators O_1 and O_2 were screwed into either end of a steel tube M . The latter was interchangeable and four samples were produced with the following values of the length m

$$m: 37, 63, 89, 115 \text{ mm.}$$

By means of the tubes and the thread in it the distance l_0 between the apertures of the two oscillators could be given prescribed values within sufficiently wide limits. The tube with the oscillators was introduced between the co-axial nozzles N_1N_2 mounted at the ends of two pipes. The latter were carried by two steel tube columns on a heavy support constituted by a piece of channel iron. On to the same was clamped a three-coordinate-slide carrying the tube M with the oscillators. It served to adjust

the position of the oscillators between the nozzles N_1N_2 after the axis of the tube had been made parallel to the common axis of the two nozzles. By means of this arrangement the two generators N_1O_1 and N_2O_2 could be made to vibrate synchronously, the synchronism being established by the ear. In the experiments to be described below three systems were used. When set for synchronism the values of l_0 and s , fig. 12, were those stated in the following review of data.

System:	1	2	3	
l_0	70	60	80	mm
s	79.5	70.0	91.0	mm
p	2.15	2.28	2.53	atm
λ	26.4	25.6	27.2	mm
Δ	$20 \cdot 10^{-2}$	$25 \cdot 10^{-2}$	$36 \cdot 10^{-2}$	mm

The review also shows the values of the joint excess pressure p at which the two generators were operated. Further the values of the joint wave-length λ and finally a quality Δ , which means the width of the interval within which the centre of the twin generator must be located—midway between the nozzles—in order to obtain synchronism. The value of Δ and the position of the interval is readily determined by means of one of the components of the three-coordinate-slide after which the twin generator is set at the centre of the interval when synchronisation is aimed at.

With the arrangement now described experimental pictures were produced of the variation of the radiation with the direction in a plane through the axis of the twin generator when the latter was set for synchronism. For this purpose the acoustic cabinet of the Laboratory of Technical Physics was used. A description of this cabinet is given in the monograph referred to on p. 3. The cabinet was furnished with two indicators for absolute measurement of acoustic radiation, viz. a Rayleigh Disk- and an Acoustic Radiometer indicator. Of these the latter apparatus was used. The twin generator was clamped to the top of a steel column mounted on a heavy carriage running on rails in the direction of the longitudinal axis of the cabinet. By means of this carriage the twin generator could be placed at any distance, within certain

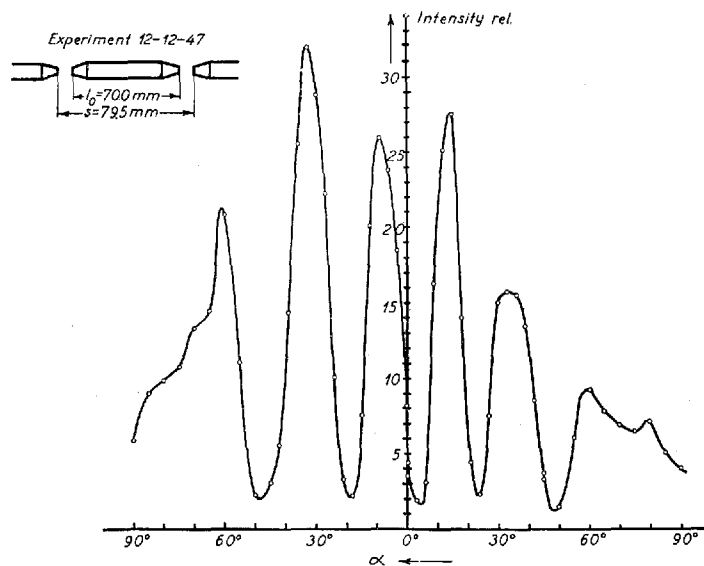


Fig. 13. Radiation from synchronised Twin Generator.
Exp. 12—12—47, $l = 74.7 \text{ mm}$, $\lambda = 25.2 \text{ mm}$.

limits, from the indicator. The line from the centre of the twin generator to the centre of the disk of the radiometer was made perpendicular to the disk when the indicator was in its zero position. Again the centre of the generator was set in the axis of the column carrying the generator. The column could be turned about this axis, and the angle of rotation could be read on a dial fastened to the column. In that way the angle α between the axis of the generator and the line to the centre of the indicator disk could be varied continuously and so the radiation from the generator could be measured for a suitable number of values of α . The details of the use of the indicator and of the indicator itself are described in another monograph from the Laboratory of Technical Physics¹. During the production of the radiation curve the excess pressure at which the twin generator is operated must be kept constant with a tolerance of a few mm Hg-column. This was done automatically by means of a suitable arrangement controlled by a mercury manometer.

¹ JUL. HARTMANN and TAGE MORTENSEN: A Comparison of the Rayleigh Disk- and the Acoustic Radiometer Methods for the Measurement of Sound Wave Energy. Ingeniørvidenskabelige Skrifter published by The Academy of Technical Sciences. Copenhagen 1948.

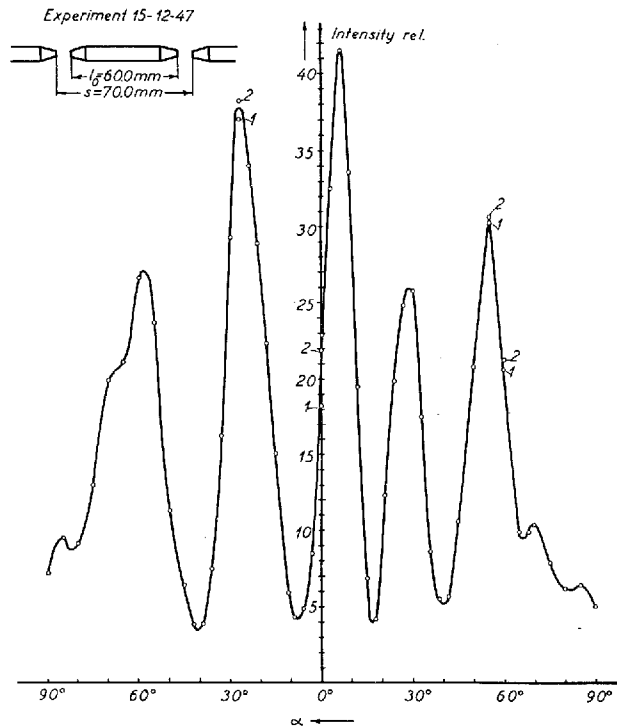


Fig. 14. Radiation from synchronized Twin Generator.
Exp. 15—12—47, $l = 65 \text{ mm}$, $\lambda = 25.7 \text{ mm}$.

Figs. 13 to 15, now, show three radiation curves for the synchronised twin generator, all produced for a distance $A = 200 \text{ cm}$ between the centre of the generator and that of the radiometer plate. The curves correspond to three values of the distance l between the acoustic centres of the two components of the twin generator. Each of these centres is assumed to be located half way between the nozzle and the front of the oscillator in question. The radiation diagrams have on the whole the shape to be expected from the simple theory indicated in fig. 16. Here G_1 and G_2 represent the two components of the twin generator visualised as two point sources of radiation $l \text{ mm}$ apart. With a uniform radiation, maxima of radiation should be measured in directions α determined by the relation

$$(1) \quad l \sin \alpha = n\lambda \quad (n: 0, 1, 2 \dots).$$

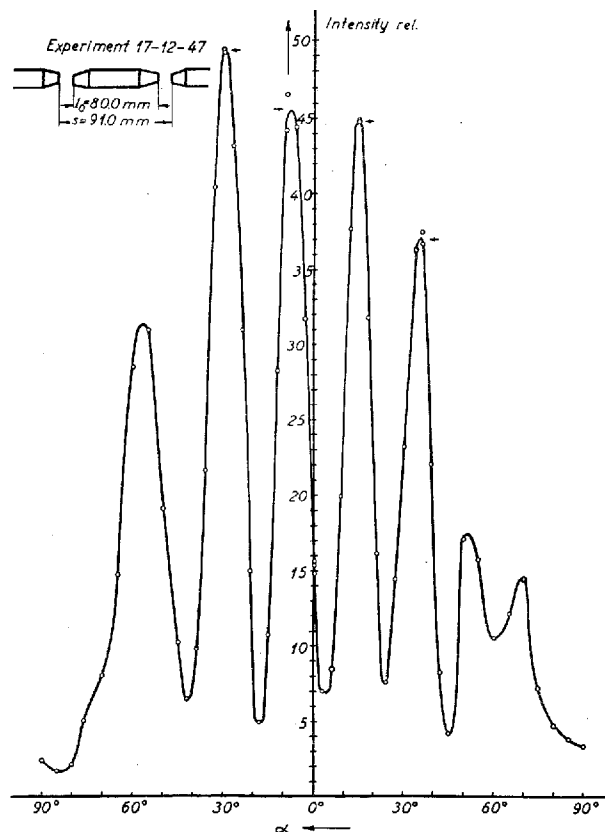


Fig. 15. Radiation from synchronized Twin Generator.
Exp. 17—12—47, $l = 85.5 \text{ mm}$, $\lambda = 27.1 \text{ mm}$.

In Table I the angles of maximum radiation as computed from this relation for $n = 1$ and $n = 2$ are compared with those derived from the observed curves. Further the observed angles α_0 corresponding to $n = 0$ are stated. It will be noted that α_0 is not zero as prescribed by the theory (1) and it is also seen that the observed values of α for $n = 1$ and $n = 2$ exceed the calculated values by 10 p.c. or more. These discrepancies are

TABLE I.

Exp.	l mm	λ mm	α_0	α_1 obs.	α_2 obs.	α_1 calc.	α_2 calc.
11—12—47 .	74.7	25.2	+7.°4	23.°0	48.°4	19.°7	42.°5
15—12—47 .	65.0	25.7	—6.°2	25.°2	59.°5	23.°3	52.°2
17—12—47 .	85.5	27.1	+6.°8	22.°2	43.°9	18.°6	39.°5

hardly to be wondered at, for the distribution of the radiation from each of the two components of the twin generator is far from being uniform. In the directions corresponding to $\alpha = -90^\circ$ and $\alpha = +90^\circ$ the radiations are zero and the largest radiation is measured not in a direction perpendicular to the axis of the generator but 10° to 20° from this directions towards the oscil-

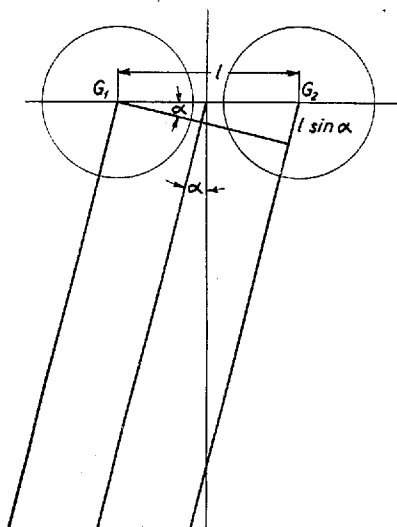


Fig. 16. To the Theory of the Radiation from the synchronised Twin Generator.

lator. (Comp. p. 3. Ref. 1. Figs. III. 24 and III. 25). In order to elucidate the effect of the inhomogeneity of radiation a graphical determination of the radiation curve for a twin generator is shown in fig. 17. The jet of component G_1 is directed from right to left, that of the component G_2 in the opposite direction. The individual radiation curves are marked G_1 and G_2 . Obviously they are symmetrical with respect to the line Oc_0 perpendicular to the axis of each of the components. They are drawn only for half of an axial plane, seeing that we are here concerned with the unilateral radiation only. Let Ob and Oc be directions determined by (1) for $n = 1$ and $n = 2$, then the amplitude recorded in these directions are simply the sums of the amplitudes of the radiations from each of the two component generators, i. e. $Oc_1 = Oa_1 + Ob_1$ resp. $Oc_2 = Oa_2 + Ob_2$. Similarly in the directions determined by $l \sin \alpha = n \cdot \lambda/2$ for $n = 1$ and $n = 3$

the resultant amplitudes are the differences between the amplitudes originating in each of the component generators. Obviously the resultant amplitude curve for the twin generator will approach the curve traced in the figure. As will be seen, the maxima are not drawn in the directions given by α_1 and α_2 and it will readily be gathered that with non-uniform radiations from the component generators the maxima need not be exactly in these directions.

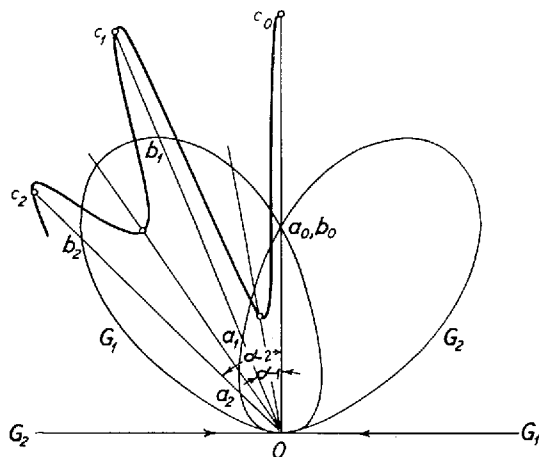


Fig. 17. Graphical Determination of the Radiation Curve from the synchronised Twin Generator.

So the differences between the observed and calculated values of α_1 and α_2 in Table I may be explained and most likely are to be explained by the said lack of uniformity. The two component generators have in fig. 17 been assumed to exhibit exactly symmetrical radiation curves. The actual components probably do not show such symmetry, and this may explain the differences between α_0 and zero or part of this difference. For, in addition, shortcomings in the determination of the zero points for the reading of α may contribute to the difference. There are other features revealed by the figs. 13—15, viz. the irregularities of the maximum or minimum ordinates, which likewise reflect lack of uniformity in the separate radiation curves. It should here be emphasised that the irregularities are real and not due to the uncertainty of the production of the curves. This fact was established by checking several points of the curves by repeated observations after the first production of the curve. The twin points 1 and 2 in fig. 14 illustrate such checking.

3. Synchronisation Experiments with independent Generators.

The next step taken was to carry out synchronisation experiments with two entirely independent generators. The generators were of the type shown in fig. 18 (Comp. p. 3. Ref. 1. Fig. I. 2). Two such generators were arranged with parallel axes on two slides which could be displaced along a common steel bar so that the axial distance l between the generators could be varied continuously from a minimum value of about 30 mm to about 260 mm. With this arrangement a number of experiments was made which will be best understood from fig. 19, representing the result of one of these experiments, viz. Exp. 16—3—48.

Both of the generators had nozzles of 6 mm diameter and oscillators the depth and width of which were both 6 mm. They were fed from the same compressor at an excess pressure of 3.00 kg/cm^2 . The first thing done was to set one of the generators, I, for maximum radiation. The distance a_I from the nozzle to the aperture of the oscillator corresponding to this radiation was found to be 7.7 mm.—Now the second generator, II, was removed to such a distance from I that a reaction between the two was precluded and then the distance a_{II} between its nozzle and oscillator was adjusted so that the two generators emitted waves of the same wave-length λ . The distance a_{IIp} thus found was assumed to represent the setting most favourable for synchronisation.—The generator II was then put out of tune by an increase of a_{II} of such a size that synchronisation could just be achieved

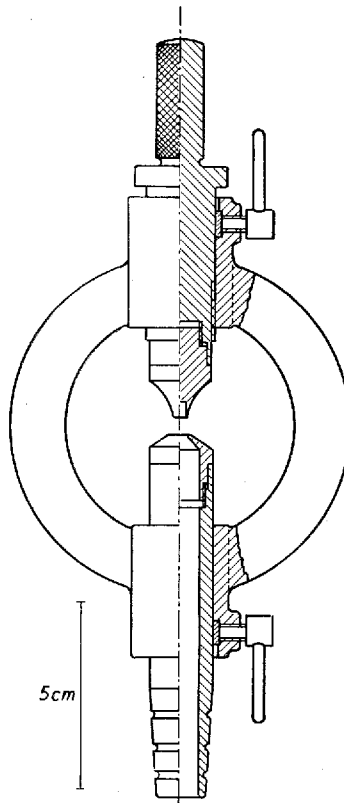


Fig. 18. Generator used in Synchronisation Experiments with separate Generators.

when the distance l was reduced to its lowest possible value, i. e. $l = 29.6$ mm. The value of a_{II} was now $a_{II0} = 7.9$ mm. In fig. 19, where l is the abscissa and where the number of the observation or group of observations is written along the axis of the ordinate, the observation referred to is represented by the single point with the abscissa 29.6 mm and the ordinate no. 1.—Next a_{II} was reduced by 0.31 mm to 7.6 mm and fresh

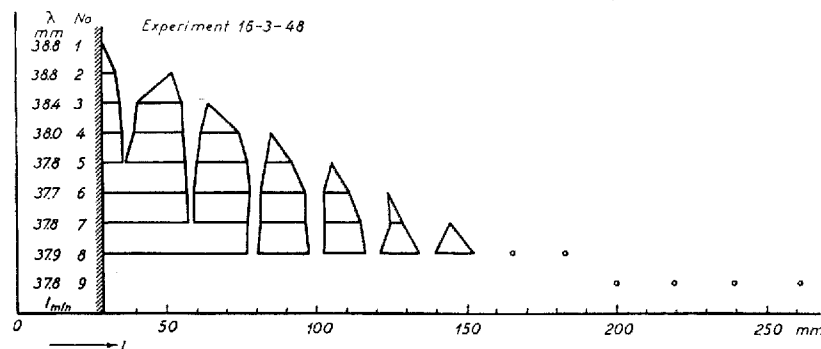


Fig. 19. Results from Synchronisation Exp. 16—3—48.

observations were made. Now synchronisation was obtained within an interval from l_{\min} to $l = 33.5$ mm and furthermore synchronisation could be produced at a single point $l = 52.1$ mm.—Again a_{II} was reduced this time to 7.45 mm. There are now two distinct intervals of synchronisation: l_{\min} to 34.8 mm and 40.5 to 55.4 mm. Further, synchronism was attained at the point $l = 64.2$ mm. The general trend of the experiment will now be quite clear. The value of a_{II} is step by step approached to that corresponding to the setting for a common wave-length. As this setting is approached the widths of the intervals of synchronisation increase and more and more of them overlap so that ultimately synchronisation is achieved for all values of the axial distance l out to say $l = 100$ mm or above. Further, synchronism is obtained at distinct points for values of l up to about 260 mm.

Quite obviously the domains of synchronisation in fig. 19 are distributed periodically, the distance between two consecutive domains being about $\lambda/2$. In the following review, l_c is the location of the centre of a domain, while l_t is the location of the top-point of the domain. The centre is taken to be the midpoint of the interval observed with the first number following that of

No.	1	2	3	4	5	6	7	8	9	10	11	12	13
l_e	29	47	68.5	89.0	109	128	146	165	182.5	200	219	239	261 mm
l_t	29	52	64	85	105	124	144	165	182.5	200	219	239	261 mm

the top-point number. Fig. 20 shows the variation of l_t with the number of the observation. The displacement is linear

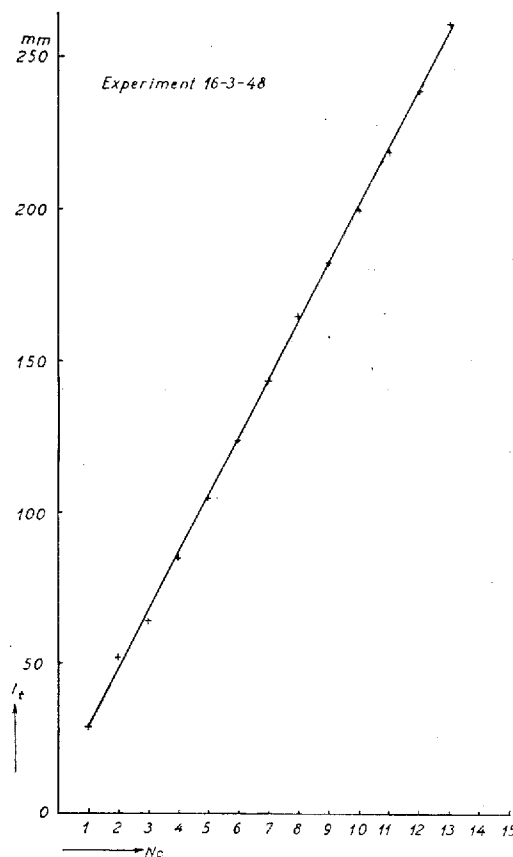


Fig. 20. Location of the Intervals of Synchronisation.

and the average distance between adjacent points of synchronisation is found to be 19.1 mm, while the value of the half-wave as found by a Kundt tube was 19.2 mm.

In an experiment preceding that shown in fig. 19, Exp. 8—3—48, and carried out with the same generator, the average distance between consecutive points of synchronisation was 19.0 mm while

$\lambda/2$ was 19.1 mm. The distance between the domains of synchronisation is thus exactly equal to half the wave-length. It should here be noted that the value of the wave-length in question

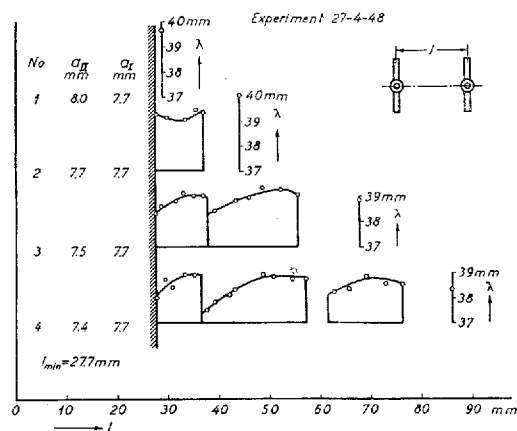


Fig. 21. Variation of the Wave-Length within the Interval of Synchronisation Exp. 27—4—48.

was that corresponding to each separate generator set for maximum radiation uninfluenced by the other generator.

After the location of the domains of synchronisation had been studied, attention was directed to the variation of the common

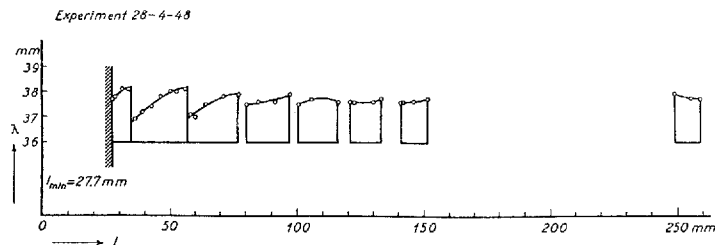


Fig. 22. Variation of the Wave-Length within the Interval of Synchronisation. Exp. 28—4—48.

wave-length within each interval of synchronisation. Two experiments made with the same generators as above are reproduced in figs. 21 and 22. (Exp. 27—4—48 and Exp. 28—4—48). In the diagrams the abscissa is again the distance l between the generators, the ordinate the number of the experiment. The latter is

characterised by the values of a , i. e. a_I and a_{II} for the two generators. These values are written in the diagram fig. 21 (not in fig. 22). The curves drawn represent the variation of the joint wave-length λ with l , scales for the reading of λ being added to each component experiment. In the cases where synchronisation was obtained at one point only, the value for λ is marked on the scale proper, which is drawn above the corresponding value of l . It is seen that λ as a rule increases with l within each interval of synchronisation reaching a maximum close to the upper boundary of the interval and then starting anew with a lower value in the following interval. If two adjacent intervals have a common frontier the value of λ will jump quite suddenly in the border line.

4. Photographs of Waves.

In the experiments now described synchronism was established either by the ear or by means of a cathode ray oscillograph connected to a crystal microphone through a suitable amplifier. In connection with the experiments presented in figs. 21–22 a series of photographs of the waves emitted from the aggregate of the two generators was produced (Exp. 29–4–48). The generators were tuned for the same wave-length, $a_I = 7.7$ mm, $a_{II} = 7.1$ mm, and so a stable synchronisation was obtained within a rather wide domain comprising the first four intervals of synchronisation. The photographs were produced with the distances l between the component generators corresponding to the centres of these four intervals, i. e. with l equal to about 29, 50, 70 and 90 mm respectively. At each distance l 5 photographs were produced corresponding to the values 0° , -10° , -20° , $+10^\circ$ and $+20^\circ$ of the angle α between the plane of symmetry of the aggregate and the line from the centre of the same to the centre of the microphone. In all cases the distance between the two centres was 100 cm. The photographs are reproduced in fig. 23, a key to the photographs being given in Table II. Obviously the waves are as a rule rather far from being purely sinusoidal containing a pronounced second harmonic (a well-known feature of the waves from the air-jet generator). The wave shape and the amplitude depend on the direction to the microphone, a fact which of course is explained by the complex con-

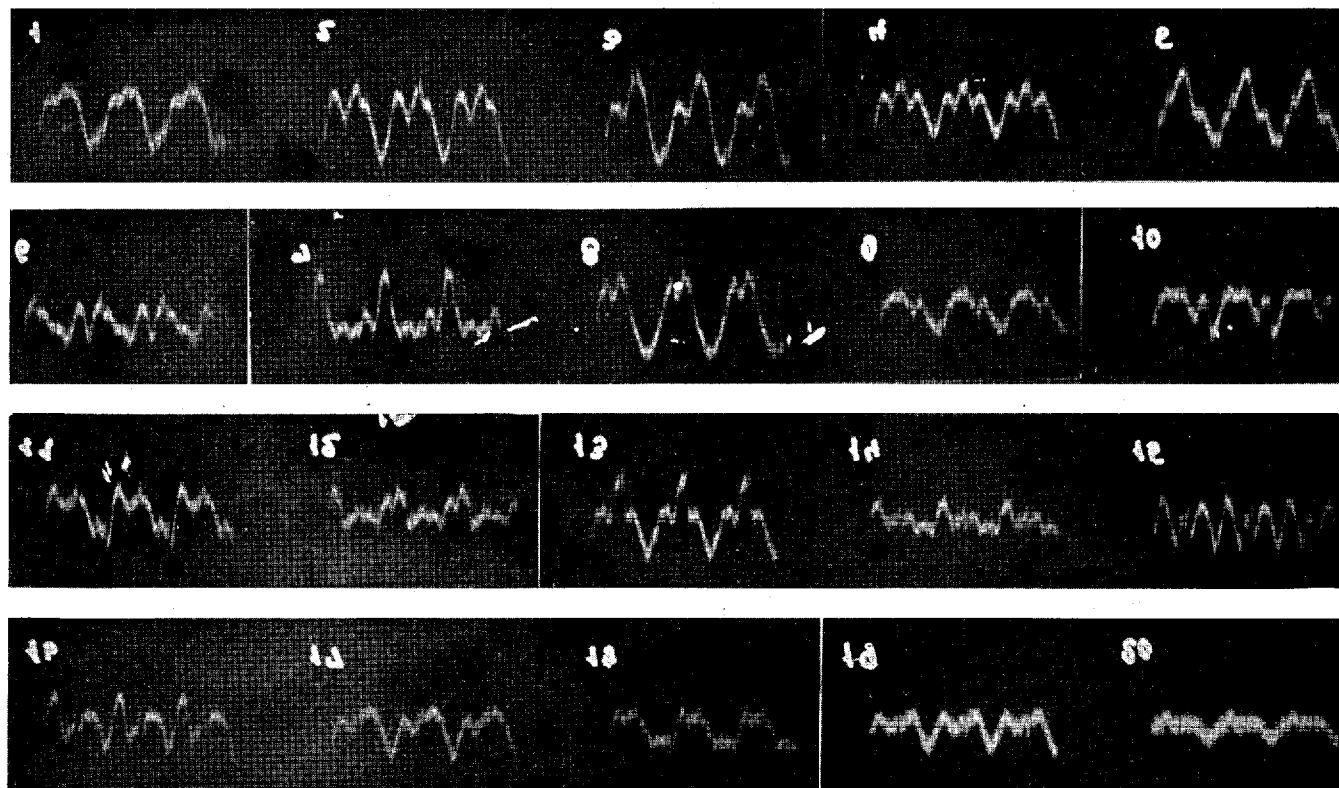


Fig. 23. Photographs of Waves from synchronised Generators. Exp. 29—4—48.

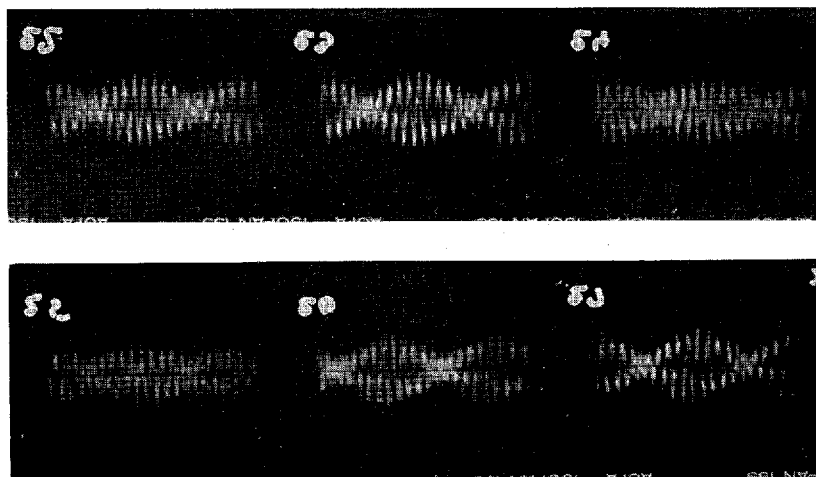


Fig. 24. Photographs of Beat Phenomena.

Nos. 22—27, $l = 81.1$ mm, $\alpha = +20^\circ$, $a_I = 7.7$ mm, $a_{II} = 8.9$ mm.

stitution of the radiation from each of the two generators and from the interference of the component waves.

When the two generators are not exactly synchronised beat phenomena are observed on the screen of the oscillograph. Fig. 24 shows examples of photographic reproductions.

TABLE II.

Number of Phot.	l mm	α degrees	λ mm
1	90.3	0	37.8
2	—	— 10	—
3	—	— 20	—
4	—	+ 10	—
5	—	+ 20	—
6	70.7	0	37.9
7	—	— 10	—
8	—	— 20	—
9	—	+ 10	—
10	—	+ 20	—
11	49.2	0	38.0
12	—	— 10	—
13	—	— 20	—
14	—	+ 10	—
15	—	+ 20	—
16	28.9	0	38.0
17	—	— 10	—
18	—	— 20	—
19	—	+ 10	—
20	—	+ 20	—

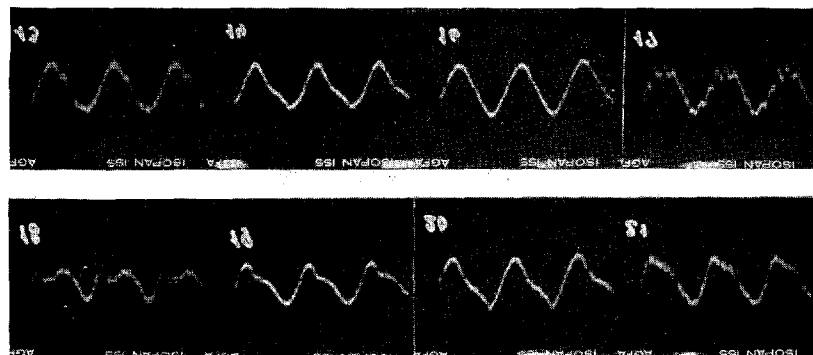


Fig. 25. Effect of Absorbent on Wave Pictures. Exp. 18—10—47.

The slight variations in the aspect of the photographs nos. 22—27 are caused by very minute variations in the α -setting of the second generator.

In connection with the oscillographic investigations now reported a series of wave pictures were produced with the aim of examining whether the very high harmonics of the waves, characteristic of the latter—in conjunction with the second harmonic—could be removed by filtration of the wave through one or two layers of a cotton-wool curtain containing 1 kg wool per m^2 . Table III in connection with the oscillograms reproduced in fig. 25 give some of the results of the investigation. (Exp. 18—10—47). In the table α indicates the distance between the nozzle and the oscillator, F is a measure of the amplification. Seeing that the absorbent would, of course, not only reduce the amplitudes of

TABLE III.

Phot. No.	Number of Layers	Excess Pressure kg/cm^2	α mm	Amplific. F	Damping of Fundamental
13	0	2.4	7	0	
14	1	2.4	7	$8 \cdot 10^3$	5.3
16	2	3.0	7	$10.1 \cdot 10^3$	
17	0	3.0	7	$8.5 \cdot 10^2$	22.0
18	0	2.4	7	$8.5 \cdot 10^2$	
19	2	2.4	7	$10.0 \cdot 10^3$	24.7
20	2	2.4	8	$10.1 \cdot 10^3$	
21	0	2.4	8	$8.5 \cdot 10^2$	21.4

the higher harmonics but also those of the fundamental and the second harmonic, a higher amplification was used in case of filtration in order to render the wave-pictures more easily comparable. Apparently there is a marked smoothing out as the effect of the filtering; it should be noted that the pictures must be compared in the way indicated in the table, i. e. no. 13 with 14, no. 16 with 17 etc. It will be seen that quite regular waves may be obtained by this method of filtering, comp. nos. 16 and 17.

APPENDIX

1. The Stem-Generator.

In connection with the synchronisation experiments described above a new form of the Hartmann generator was developed. It is shown in figs. 1—2 and like the ordinary form comprises a nozzle *N* and a cylindrical oscillator *O*. The latter is, however,

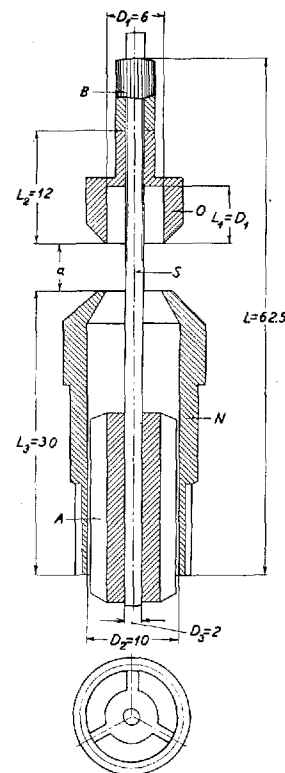


Fig. 1. The Stem-Generator.

coupled to the nozzle by means of a rod, the stem *S*, coaxial with both of the two members. On this stem the oscillator can be displaced, a thread being cut in the surface of the stem and a corresponding thread in a bore through an extension of the oscillator member. In this way the latter is set in the proper position relatively to the nozzle after which setting the position is secured by means of a lock nut *B*. The stem is safely clamped to the nozzle member by means of a cylinder *A* pressed into the nozzle. In the surface of the cylinder three grooves are cut through which the compressed air feeding the jet will flow to the aperture of the nozzle. The constructional merits of the generator are obvious. The heavy coupling between the jet-pipe or nozzle and the oscillator has been avoided and the production of the generator thereby greatly simplified. The space occupied by the source proper of the sound waves has been reduced to a mini-

mum, a considerable advantage in many applications, particularly perhaps in the production of intensive wave-fields of large extensions by means of a great number of synchronised generators. It was the latter application which inspired the new generator. In the synchronisation experiments it did not compete

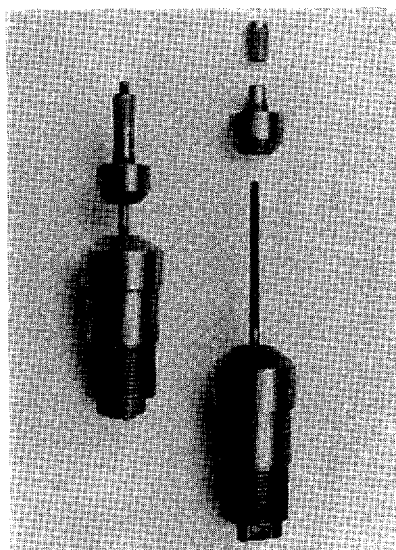


Fig. 2. The Stem-Generator.

too well with the older type. Nevertheless the system would seem of considerable interest, exhibiting certain features of its own. So it was made the subject of a fairly comprehensive investigation, the main results of which will now be reported.

2. The Performance of the Stem-Generator.

Figs. 3 a—d show characteristics of the stem-generator for the excess pressures 0.5, 1.0, 1.5 and 2.0 kg/cm². The diagrams in the first instance illustrate the variation of the volume density E erg/cm³ of the radiation with the direction in a plane through the axis of the generator, α being the angle between the direction in question and the axis reckoned positive from the nozzle to the oscillator. In addition the variation of E with the distance a from the nozzle to the oscillator is presented, and finally the

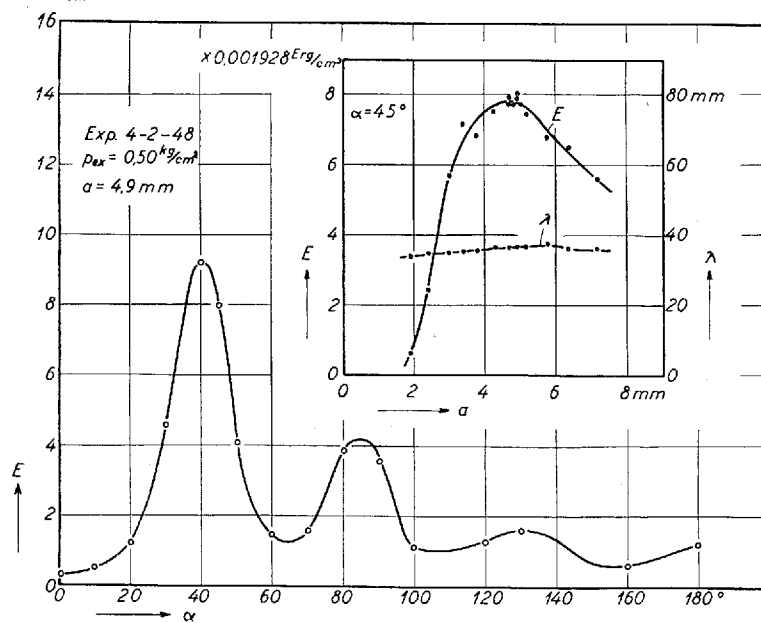
$\times 0,001928 \text{ Erg/cm}^2$


Fig. 3 a.

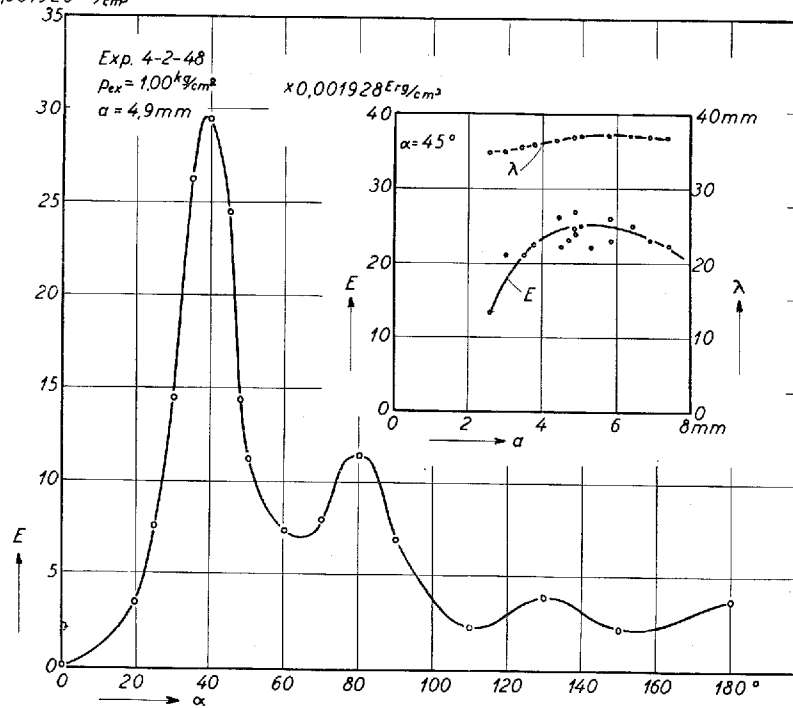
 $\times 0,001928 \text{ Erg/cm}^2$


Fig. 3 b.

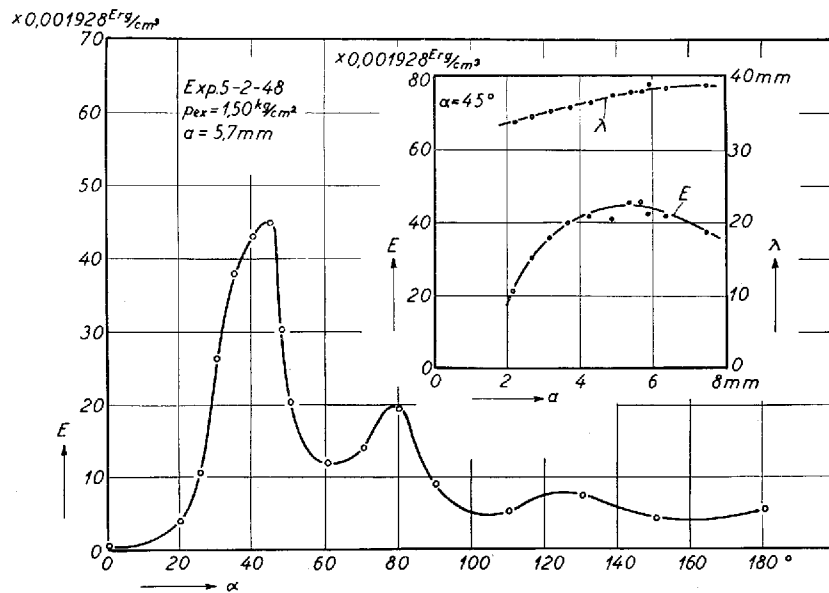


Fig. 3 c.

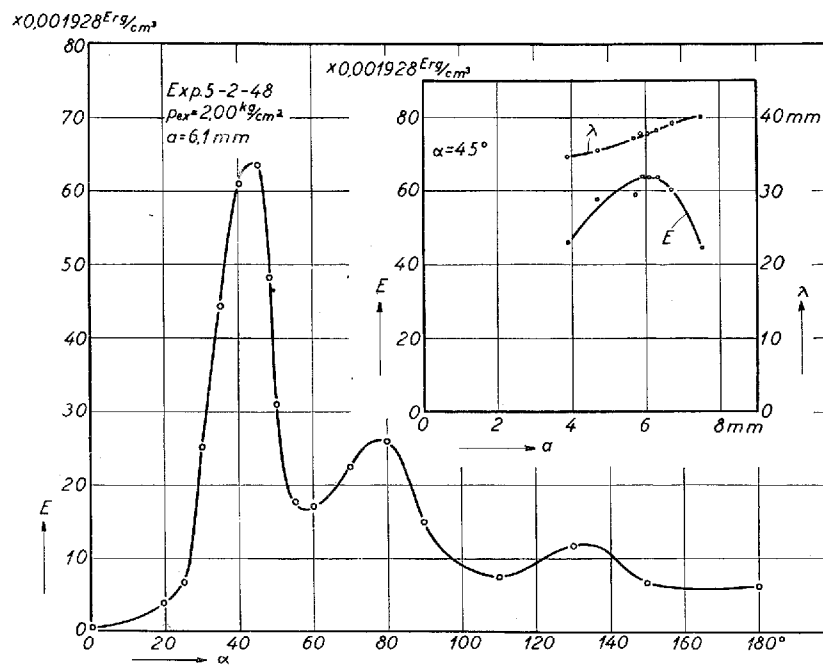


Fig. 3 d.

wave-length λ as a function of α . The two latter variations correspond to the direction of maximum radiation or nearly so, i. e. to $\alpha = 45^\circ$.

It should first of all be noted that the stem-generator will operate below the critical excess pressure of about 1 kg/cm², i. e. with a jet of a velocity below that of sound. In that respect it deviates markedly from the ordinary Hartmann Generator, the operation of which distinctly depends on a jet of supersonic velocity and finds its explanation in the structure of such a jet. Again the distribution of intensity round the stem-generator is more regular than is generally the case with the earlier generator. All the curves in figs. 3 a—d were derived from absolute measurements of the intensity, carried out in a cabinet with absorbing walls by means of a radiometer *Ph-1a/S-4*. The values of E with this indicator are computed from a formula

$$E = 0.001928 D \text{ erg/cm}^3$$

where D cm is the reading on the hand wheel of the indicator by which the radiometer was set at each measurement.¹ From the E - α -curves in fig. 3 a—d the total radiation of acoustic energy, as measured at a distance $S = 200$ cm from the generator, could be derived by a numerical integration.

TABLE I. *Performance of 6 mm Stem-Generator.*

Exp.	$p_{\text{ex.}}$ kg/cm ²	a mm	λ mm	E_{max} erg/cm ³ rel.	$I_{\text{obs.}}$ Watt	$I_{\text{cor.}}$ Watt	I_c Watt	η p.c.
4—2—48 ...	0.50	4.9	36.3	9.2	8.1	9.45	270	3.5
4—2—48 ...	1.00	4.9	36.8	29.5	25.0	29.0	710	4.1
3—2—48 ...	1.50	5.7	38.0	45.0	33.5	39.2	1270	3.1
3—2—48 ...	2.00	6.1	37.7	63.5	58.8	68.8	1910	3.6
8—1—48 ...	2.90	4.0	31.5	77.0	103	121	3200	3.8

In Table I the main results of the investigation are stated. Here $p_{\text{ex.}}$ is the excess pressure in the container from which the generator is fed, a the distance from the nozzle to the aperture of

¹ A description of the indicator and of its operation is given in the monograph: JUL. HARTMANN and TAGE MORTENSEN: A Comparison of the Rayleigh Disk- and the Acoustic Radiometer Methods for the Measurement of Sound Wave Energy, published by the Academy of Technical Sciences, Ingeniørviden-skabelige Skrifter 1948 No. 2. Copenhagen 1948.

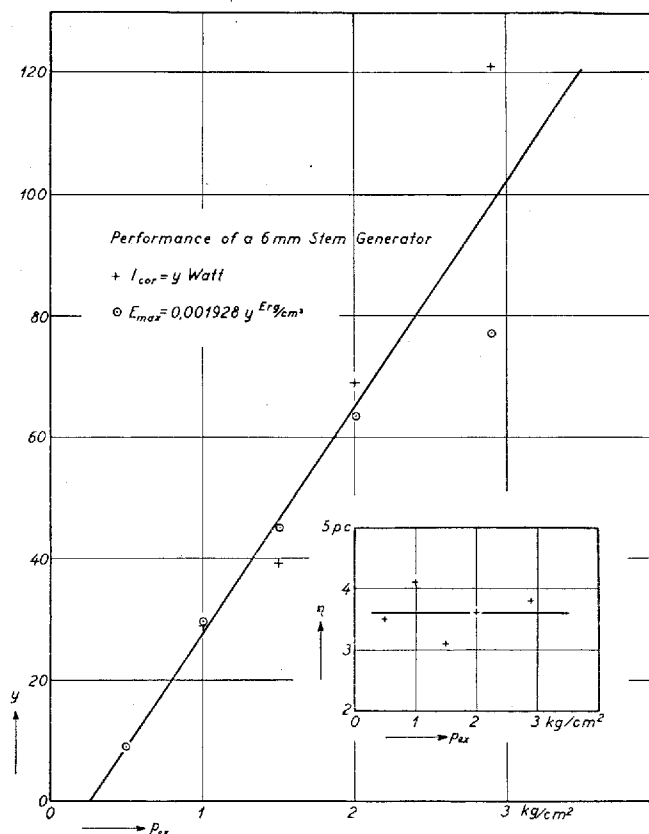


Fig. 4. Variation of Maximum Intensity of Radiation E_{max} , erg/cm^2 , and of the total Radiation, Watt, with the Excess Pressure p_{ex} , kg/cm^2 .

the oscillator. E_{max} is the maximum ordinate of the radiation curve and $I_{obs.}$ the total acoustic radiation as found from the radiation curves by numerical integration. Again $I_{cor.}$ is found from $I_{obs.}$ by increasing the latter value by 17 p.c. The correction takes into account the absorption in the air and in 6 layers of gauze introduced between the generator and the indicator in order to protect the latter against air currents. Each layer was found to absorb about 2 p.c. of the radiation.

Fig. 4 shows the variation of E_{max} and $I_{cor.}$ with the excess pressure p_{ex} , kg/cm^2 . It would seem that both of the two qualities vary linearly with p_{ex} , and that they become zero at an excess pressure of about 0.3 kg/cm^2 thus at an excess pressure

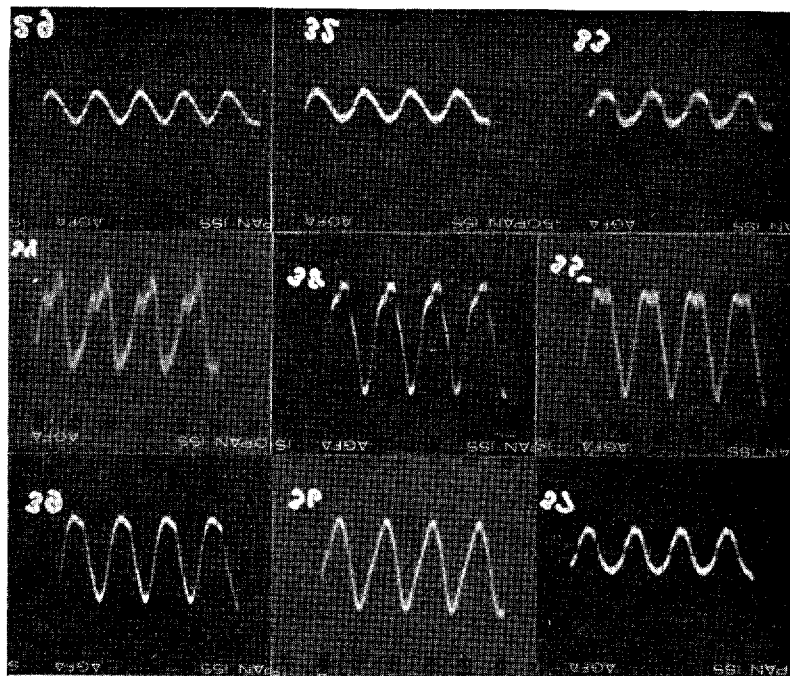


Fig. 5. Waves emitted from the Stem-Generator. Exp. 29—4—48.

well below the critical excess pressure 0.9 kg/cm^2 , at which the radiation from an ordinary Hartmann generator ceases when the excess pressure is reduced. Again, with the latter generator the total radiation is proportional to $\sqrt{p_{\text{ex.}} - 0.9}$ not to $p_{\text{ex.}} - 0.3$, another marked difference between the two generators.

In connection with the production of wave oscillograms originating in the ordinary Hartmann generator, Exp. 29—4—48, similar oscillograms were obtained for the 6 mm stem-generator at an excess pressure $p_{\text{ex.}} = 3.00 \text{ kg/cm}^2$ and with the generator set for $a = 4.0 \text{ mm}$. A series of oscillograms are reproduced in fig. 5 corresponding to the values of α stated below:

Oscillogr. No:	29	32	33	34	38	35	39	36	37
α	0	5	10	20	30	40	60	80	120°
$2A$	3.5	3.5	4.0	13.0	14.0	13.0	10.5	11.0	5.0
$4A^2$...	12.2	12.2	16.0	169	196	169	110	121	25

The waves would seem rather more regular than those from the ordinary generator. The double amplitude $2A$ was measured on

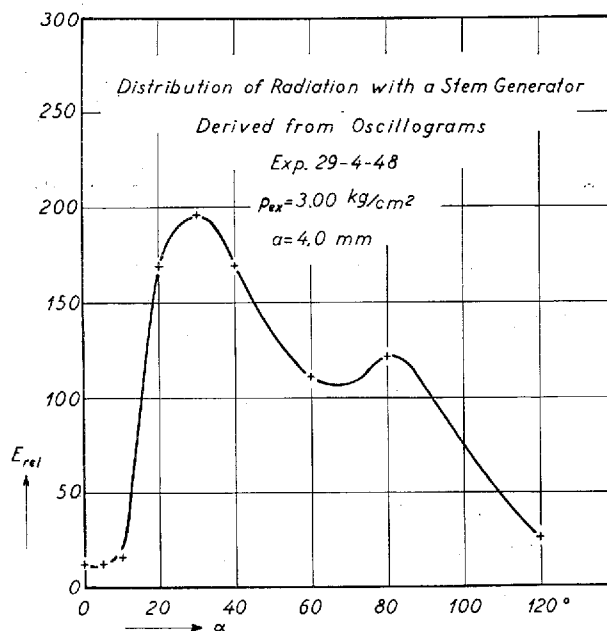


Fig. 6. Distribution of Radiation with a Stem-Generator derived from Oscillograms.

the oscillograms. In fig. 6 the squares $4A^2$ are plotted against α . The curve found should picture the variation of the intensity of radiation with the direction. It may be compared to the directly observed radiation curve fig. 3 d which, however, corresponds to the excess pressure $p_{ex} = 2.00 \text{ kg/cm}^2$. Quite obviously the curve in fig. 6 has the main features in common with the curve in fig. 3 d.

3. The Pulsation Phenomenon with the Stem-Generator.

If the oscillator of the ordinary Hartmann Generator is replaced by a nozzle, similar to the main nozzle, connected through a rubber tube to a steel bottle of suitable size, the so-called pulsation phenomenon is observed, characterised by the bottle alternately taking in and discharging air. In order to repeat the pulsation experiment with the nozzle of a stem-generator, the oscillator was removed and the stem was passed axially into the nozzle of the pulsator as indicated in fig. 7 a, where N_1 is the main nozzle with the stem S and N_2 the pulsator nozzle.

In some experiments the opposite arrangement was used, i. e. the nozzle with the stem was employed for the pulsator while the main nozzle was an ordinary jet-hole. The pulsation phenomenon was studied by means of the multiple slit Schlieren-Bench. The main results may be thus stated.

In the first instance it turned out that pulsations were obtained with excess pressures p as low as 0.5 kg/cm^2 , and with both of the two applications of the stem-nozzle.

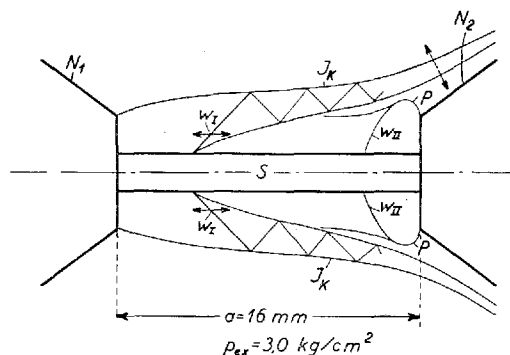


Fig. 7 a. The Pulsation Experiment with the Stem-System.

Fig. 7 a. shows a drawing of the jet during the phase of discharge. The joint value of the diameters of the two nozzles was 6 mm, the diameter of the stem was 2 mm and the excess pressure $p_{ex.}$ employed was 3.0 kg/cm^2 . If the distance a between N_1 and N_2 was less than 16 mm no pulsations were observed; at $a = 16 \text{ mm}$ the pulsations started, their frequency was, with a bottle of about 10 dm^3 , nearly 2 Hz, i. e. of the same order of size as with the ordinary pulsator with two nozzles of 6 mm diameter. The air from the two colliding jets, the main jet and the pulsator jet, escapes in a bell-shaped flow J_K enveloping the pulsator jet and the pulsator nozzle. A conical shock-wave W_I appears in the main jet apparently forming one of the boundaries of the collision-zone. The other boundary, if formed, is not seen. Obviously J_K represents, with the excess pressure stated, a supersonic flow for shock-waves are distinctly seen in it with an aspect approximately as indicated. Close to the circumference of the nozzle N_2 an annular protuberance P is observed in the Schlieren picture. At the very first moment of the discharge a faint shock-

wave W_{II} is seen in continuation of the contour of this protuberance. During the discharge it moves in the direction of N_1 but disappears very soon. During the whole period of the pulsation phenomenon oscillatory movements of the various features of the picture, particularly of W_I and J_K , are observed. Their size and the direction of the oscillations are indicated by the arrows in fig. 7a.

Now, if the excess pressure $p_{ex.}$ is reduced the distance a from the main nozzle at which the pulsations start is reduced as

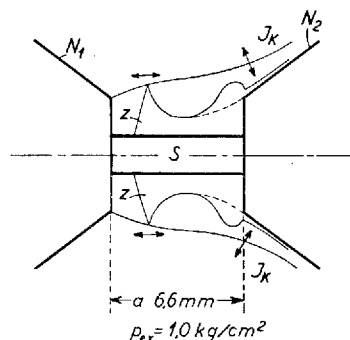


Fig. 7 b. The Pulsation Experiment with the Stem-System.

indicated in fig. 7b corresponding to $p_{ex.} = 1 \text{ kg/cm}^2$ and to the first moment of the phase of discharge. The aspect of the jet is, otherwise, not very different from that corresponding to $p_{ex.} = 3 \text{ kg/cm}^2$ and the frequency of the pulsations was of the same order of size as before. But so close to the critical excess pressure of about 0.9 kg/cm^2 all traces of shock-waves had disappeared from the collision-jet J_K and, it would seem, also from the main jet. Again oscillations as indicated by arrows were observed.

With still lower values of the excess pressure, 0.8 and 0.5 kg/cm^2 , the pulsations continued with about the same frequency. The picture of the jet resembled that reproduced in fig. 7b, however, with reduced sharpness of the feature Z . In the case of $p_{ex.} = 0.5 \text{ kg/cm}^2$ the pulsations started with $a = 8.9 \text{ mm}$ and continued within an interval of several millimeters above this limit. Quite obviously the pulsation phenomenon with the stem-pulsator not only calls for a closer study of the phenomenon proper but also and in particular for an interpretation that will account for the pronounced difference from the pulsations with the ordinary full-jet pulsator.

4. Synchronisation of Stem-Generators.

Synchronisation experiments of the same type as were described for ordinary Hartmann Generators were carried out with

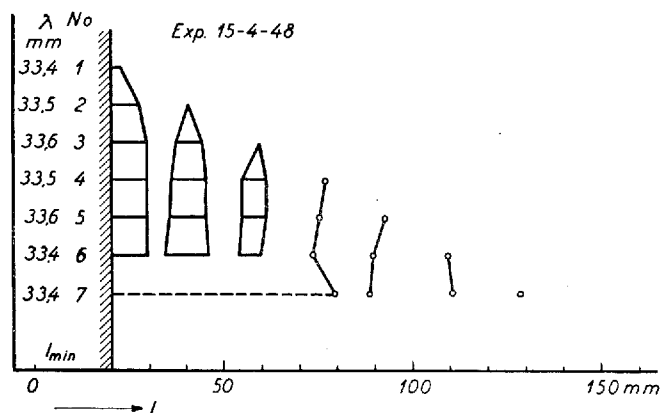


Fig. 8. Synchronisation Experiment with 6 mm Stem-Generators.

the stem-generators. The technique of the investigation was the same in the two cases so reference should be made to the earlier experiments. Fig. 8 shows the results of Exp. 15—4—48 in which two 6 mm generators were used operated at an excess pressure $p = 3.00 \text{ kg/cm}^2$. The setting of one of the generators was kept constant with the distance $a_I = 4.0 \text{ mm}$ between the nozzle and the aperture of the oscillator. The setting of the second generator was changed in seven steps from $a_{II} = 4.1 \text{ mm}$ to $a_{II} = 3.7 \text{ mm}$, the former setting corresponding to No. 1 in fig. 8 the latter to No. 7 with which setting the two generators practically were in tune. As with the ordinary Hartmann generators more and more intervals of synchronisation are found when the value a_{II} corresponding to perfect equality of frequency is approached. It would, however, seem that synchronism is less readily achieved with the stem-generators out of tune than was the case with the ordinary generators. As a matter of fact the synchronisation in the "intervals" beyond the three to the left in fig. 8 was rather uncertain, or rather, no definite limits to these intervals could be established. The joint wave-length of the synchronised waves was practically the same at all settings. From fig. 8 the average

distance between adjacent intervals is found to be 17.5 mm (distance between top-points) while the average value of $\lambda/2$ was about 16.8 mm.

The younger of the Authors of the two papers here presented is indebted to the Academy of Technical Sciences Copenhagen and the Tuborg Foundation for the grant of a Fellowship which enabled him to find the time required for carrying out his part of the work.

*The Laboratory of Technical Physics.
The Technical University of Denmark.
December 1950.*
